

What ZTF Saw Where Rubin Looked: Anomaly Hunting in DR23

MARIA V. PRUZHINSKAYA,¹ ANASTASIA D. LAVRUKHINA,¹ TIMOFEY A. SEMENIKHIN,^{2,1} ALINA A. VOLNOVA,³
SREEVARSHA SREEJITH,⁴ VADIM V. KRUSHINSKY,⁵ EMMANUEL GANGLER,⁶ EMILLE E. O. ISHIDA,⁶ MATWEY V. KORNILOV^{1,7}
AND KONSTANTIN L. MALANCHEV⁸

THE SNAD TEAM

¹*Sternberg astronomical institute, Lomonosov Moscow State University, Universitetsky pr. 13, Moscow, 119234, Russia*

²*Lomonosov Moscow State University, Faculty of Physics, Leninskie Gory, 1-2, Moscow, 119991, Russia*

³*Space Research Institute of the Russian Academy of Sciences (IKI), 84/32 Profsoyuznaya Street, Moscow, 117997, Russia*

⁴*Physics Department, University of Surrey, Stag Hill campus, Guildford, GU2 7XH, UK.*

⁵*Laboratory of Astrochemical Research, Ural Federal University, Ekaterinburg, ul. Mira d. 19, Yekaterinburg, 620002, Russia*

⁶*Université Clermont Auvergne, CNRS/IN2P3, LPC, F-63000 Clermont-Ferrand, France*

⁷*National Research University Higher School of Economics, 21/4 Staraya Basmannaya Ulitsa, Moscow, 105066, Russia*

⁸*The McWilliams Center for Cosmology & Astrophysics, Department of Physics, Carnegie Mellon University, Pittsburgh, PA 15213, USA*

ABSTRACT

We present results from the SNAD VIII Workshop, during which we conducted the first systematic anomaly search in the ZTF fields also observed by LSSTComCam during Rubin Scientific Pipeline commissioning. Using the PineForest active anomaly detection algorithm, we analysed four selected fields (two galactic and two extragalactic) and visually inspected 400 candidates. As a result, we discovered six previously uncatalogued variable stars, including RS CVn, BY Draconis, ellipsoidal, and solar-type variables, and refined classifications and periods for six known objects. These results demonstrate the effectiveness of the SNAD anomaly detection pipeline and provide a preview of the discovery potential in the upcoming LSST data.

Keywords: Time domain astronomy (2109) — Supernovae (1668) — Time series analysis (1916) — Transient detection (1957)

1. INTRODUCTION

The advent of large astronomical data sets, which took place in the last few decades, changed significantly how researchers interact with the data. In all areas of observational astronomy, communities were obliged to adapt to unprecedented volumes of photometric observations. It is safe to say that one of the areas most impacted by this new paradigm was the discovery of new, and sometimes unpredicted, astrophysical phenomena. Serendipitous discovery has become more unlikely with each new survey, which boosted the use of automatic machine learning techniques. The situation is even more drastic when we take into account expected data of the Legacy Survey of Space and time from the Vera C. Rubin Observatory (LSST Science Collaboration et al. 2009).

In order to enable systematic search for unpredicted, scientifically interesting, phenomena in large data sets, the SNAD team⁹ (A. A. Volnova et al. 2024) has been developing a series user-friendly anomaly detection (AD) tools (K. Malanchev et al. 2023; M. V. Kornilov et al. 2025) whose goal is to enable seamless interaction between the expert and the machine, and thus optimize the search for novelty in astronomical data. The pipeline has already proven to be successful in scrutinizing data from the Zwicky Transient Facility¹⁰ (ZTF; E. C. Bellm et al. 2019) under a series of different circumstances, including searches for supernovae (P. D. Aleo et al. 2022; M. V. Pruzhinskaya et al. 2023) and stellar flares (A. S. Voloshina et al. 2024), as well as the identification of artifacts in astronomical data (T. A. Semeníkhin et al.

Corresponding author: Maria Pruzhinskaya
pruzhinskaya@gmail.com

⁹ <https://snad.space/>

¹⁰ <https://www.ztf.caltech.edu/>

2025; S. Sreejith et al. 2025). We start now to redirect this experience towards a new paradigm.

In this work, we present results from the first systematic anomaly search in fields observed by both, ZTF and the LSST commissioning camera (LSSTComCam, L. P. Guy et al. 2025). We applied the SNAD pipeline to ZTF Data Release 23 (DR23) light curve data, limited to regions targeted during the on-sky campaign of the LSSTComCam dedicated to the commissioning of its Science Pipelines. Recent reports already presented result from variability search within LSST proprietary data covering the same area (K. Malanchev et al. 2025; J. L. Carlin et al. 2025; Y. Choi et al. 2025), however, to our knowledge, a similar AD search was never specifically targeted to these fields.

LSSTComCam is the Rubin Observatory’s engineering camera, used for testing and validating the observatory systems prior to the installation of the full LSST Camera (A. Roodman et al. 2024; T. Lange et al. 2024). Its focal plane consists of a single raft with a 3×3 mosaic of $4K \times 4K$ ITL science sensors, totaling 144 million pixels. It shares the same plate scale as the LSSTCam (0.2 arcsec/pixel) and covers a field of view of 40×40 arcmin. Observations with LSSTComCam were conducted at the end of 2024. For the Science Pipelines commissioning campaign, seven target fields were selected¹¹. These fields cover a total area of approximately 15 square degrees. The photometric data from 1791 LSSTComCam exposures formed the Rubin Data Preview 1 (DP1) dataset (NSF-DOE Vera C. Rubin Observatory 2025). Among the seven LSSTComCam target fields, four overlap with the ZTF footprint (see Table 1). Figure 1 shows the spatial footprint of these selected fields overlaid on ZTF coverage.

In what follows, data selection is described in Section 2; the algorithm used for anomaly search is given in Section 3; a summary of our findings is shown in Section 4 and our conclusions are discussed in Section 5.

2. DATA

We used data from the latest ZTF data release (DR23), covering the time range of $58178 \leq \text{MJD} \leq 60125$, which corresponds to March 2018 through June 2023 (E. C. Bellm et al. 2019). From this dataset, we selected only *zr*-band light curves that satisfy the quality flag criterion `catflags = 0`, holding at least 100 detections and overlapping with Rubin commissioning fields.

Feature extraction from ZTF light curves was performed using the `light-curve`¹² package, a time-series

feature extraction tool developed as part of the SNAD pipeline (K. L. Malanchev et al. 2021; A. Lavrukhina & K. Malanchev 2023). The resulting dataset contains 47 statistical features per object; the full list of features and the feature-extracted dataset are available on-line¹³.

LSSTComCam covers a significantly smaller area than a single ZTF observation field of view of 47 square degrees. Therefore, from the ZTF fields overlapping with a corresponding LSSTComCam target field, we extracted objects likely to also be observed by Rubin. However, the employed LSSTComCam observation strategy involved a complex pattern of random translational and rotational dithers around each field’s nominal pointing center, making the exact footprint non-trivial to define.

Since LSSTComCam coverage maps are not publicly available in a machine-readable form, we used Fig. 3 of L. P. Guy et al. (2025) for the region selection. We applied a percentile-based intensity thresholding to identify dark regions corresponding to observational coverage in this figure, with the percentile threshold manually selected for each image to optimize region detection. A distance transform algorithm was then used to determine the maximum inscribed circle within the primary observation region, and to estimate the radius of the corresponding field (Fig. 2).

The radius of each LSSTComCam target field and the number of ZTF objects within the footprint of these fields is given in Table 1.

3. METHODS

We applied the PineForest algorithm, implemented in the `coniferest` library (M. V. Kornilov et al. 2025), to independently explore potential outliers in each of the four fields.

PineForest is an active AD framework developed by the SNAD team. It is based upon the well-known Isolation Forest algorithm (F. T. Liu et al. 2008), which adapts the decision tree method (L. Breiman 2001; W.-Y. Loh 2014; E. B. Hunt et al. 1966) for outlier detection by exploiting the idea that anomalies tend to be more easily isolated in feature space. PineForest allows the personalization of the structure of the forest by selecting only random trees that agree with the anomaly definition informed by the user.

For each field, we conducted two PineForest sessions with a labelling budget of 50, retraining the model between iterations to incorporate expert feedback and refine the anomaly ranking.

Our main findings are summarized in the next sections.

¹¹ <https://sitcomtn-149.lsst.io/>

¹² <https://github.com/light-curve/light-curve-python>

¹³ <https://snad.space/features/>

Table 1. Coordinates, radii and names of selected LSSTComCam fields. **N** is number of ZTF objects within the footprint of these fields.

Field Code	Field Name	RA (deg)	Dec (deg)	Radius (deg)	N
Rubin SV 38 7	Low Ecliptic Latitude Field	37.86	+6.98	0.7	6758
ECDFS	Extended Chandra Deep Field South	53.13	-28.10	0.6	546
Rubin SV 95 -25	Low Galactic Latitude Field	95.00	-25.00	0.5	10649
Seagull	Seagull Nebula	106.23	-10.51	0.5	24480

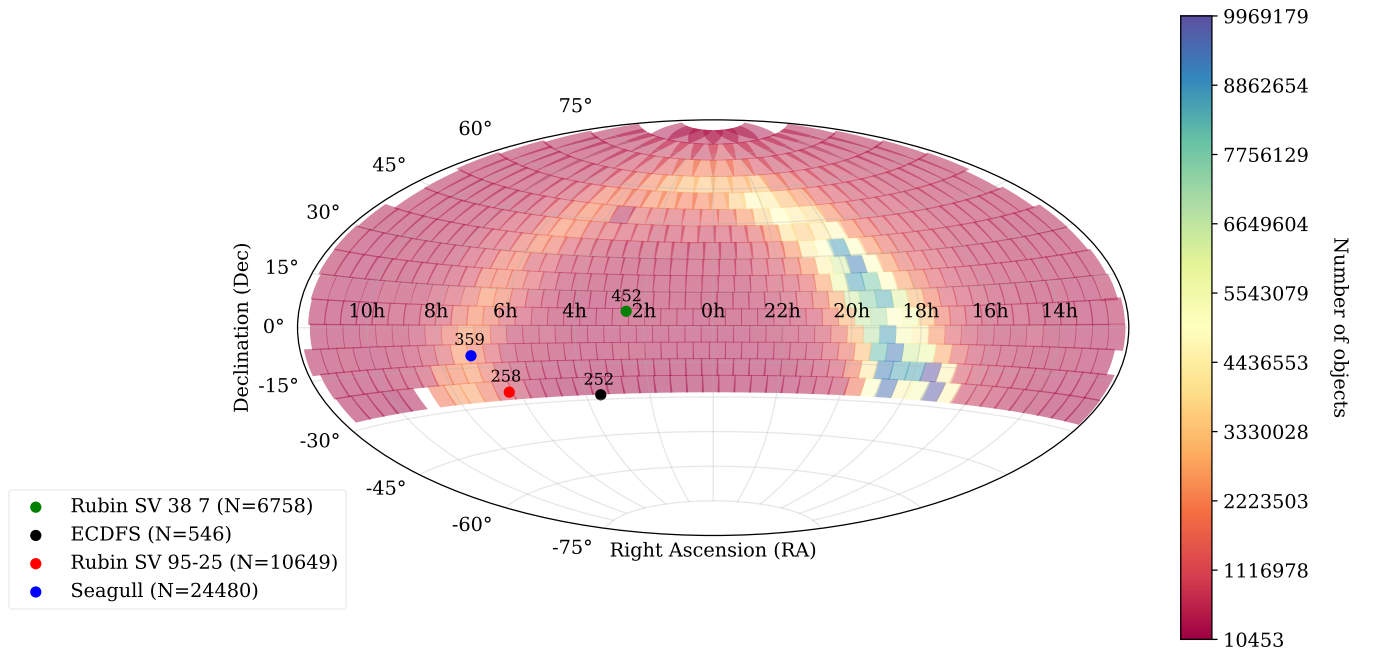


Figure 1. Spatial footprint of the four LSSTComCam target fields (circles) overlaid on ZTF sky coverage. Above each circle, the FIELDID of the corresponding overlapping ZTF field is shown. In the legend, the number in parentheses indicates how many ZTF objects fall within the respective LSSTComCam target field. The background grid outlines the ZTF observed fields. Each is colour-coded according to the number of ZTF objects in it.

4. RESULTS

We analysed, two extragalactic (Rubin SV 387 and ECDFS) and two galactic (Rubin SV 95–25 and Seagull) fields. All of which contain a certain amount of artifacts and spurious data.

The galactic fields include a wide range of variable stars, such as eclipsing binaries (EB), RR Lyrae, RS CVn systems, long-period variables (LPV), cataclysmic variables (CV), and other known and unknown variable objects. Additionally, the Seagull field, located within a nebula, also contains a dozen young stellar object (YSO) candidates, consistent with previous studies showing that YSOs preferentially reside in star-forming regions and molecular clouds (e.g., C. J. Lada & E. A. Lada 2003; N. J. Evans et al. 2009).

The extragalactic fields contain several extended sources. In these fields, we primarily found active galactic nuclei (AGN), including quasars (QSO) and one blazar candidate (ZTF OID 452216400005600), one possible supernova (AT 2022zgk), and three known asteroids (Patsy, 2003 SN65, and 2015 GZ65). A small number of stellar variables, such as RS CVn stars and EB, are also present in the extragalactic fields.

Below, we present newly identified variable stars, as well as known variables for which we refined the classification and measured periods. The periods were initially estimated using values provided in the SNAD ZTF Viewer¹⁴ (K. Malanchev et al. 2023). It uses a period corresponding to the highest Lomb-Scargle periodogram peak (N. R. Lomb 1976; J. D. Scargle 1982). These preliminary estimates were subsequently fine-tuned using the Variability Search Toolkit (VaST; K. V. Sokolovsky & A. A. Lebedev 2018). VaST employs methods developed by J. Lafler & T. D. Kinman (1965) and T. J. Deeming (1975).

4.1. *New variables*

All objects presented below are new variables that are not listed in the Gaia DR3 Variability Catalog (Gaia Collaboration et al. 2023) or other known catalogs of variable stars, including the General Catalog of Variable Stars (GCVS, N. N. Samus' et al. 2003, 2017), the International Variable Star Index (AAVSO VXS, C. L. Watson et al. 2006), the Large-amplitude variables in Gaia DR2 (N. Mowlavi et al. 2021) or the Stellar variability catalog from Gaia DR3 (J. Maíz Apellániz et al. 2023).

Each of these objects has been added to the SNAD Catalog¹⁵ and assigned a SNAD name.

4.1.1. *SNAD273*

The star ZTF OID 452216100008087 (Gaia DR3 19492077713298944) is located at equatorial coordinates $\alpha = 02^{\text{h}} 30^{\text{m}} 24.828^{\text{s}}$, $\delta = +07^{\circ} 28' 8.44''$.

The field is extragalactic, but the object is classified as a star by different surveys (e.g., R. Ahumada et al. 2020; K. J. Duncan 2022). Gaia data suggest that it is a main-sequence star, with a photogeometric distance of 959_{-70}^{+87} pc (C. A. L. Bailer-Jones et al. 2021).

The ZTF light curve (Fig. 3a), as well as Pan-STARRS1 DR2 photometry (K. C. Chambers et al. 2016; H. A. Flewelling et al. 2020), reveal low-amplitude, non-periodic variability consistent with solar-type activity.

4.1.2. *SNAD274*

The star ZTF OID 359205200010128 (Gaia DR3 3046542589365461376) is located at $\alpha = 07^{\text{h}} 04^{\text{m}} 34.577^{\text{s}}$, $\delta = -10^{\circ} 18' 10.01''$. The photogeometric distance is estimated to be 1313_{-108}^{+151} pc (C. A. L. Bailer-Jones et al. 2021). According to Gaia data, the star lies above the main sequence, suggesting it could be a rotating ellipsoidal variable (ELL).

The ZTF folded light curve is shown in Fig. 3b. The estimated period is $P = 15.2395$ days.

4.1.3. *SNAD276*

The ZTF OID 359205200015003¹⁶ (Gaia DR3 3046517850352071040) is located at $\alpha = 07^{\text{h}} 04^{\text{m}} 38.191^{\text{s}}$, $\delta = -10^{\circ} 31' 58.69''$. The photogeometric distance is estimated to be 970_{-147}^{+242} pc (C. A. L. Bailer-Jones et al. 2021).

The ZTF folded light curve is shown in Fig. 3c. The estimated period is $P = 6.34625$ days. The presence of outlier points in the light curve may indicate chromospheric activity, which is also typical for RS CVn-type stars.

4.1.4. *SNAD277*

The ZTF OID 359205200019542 (Gaia DR3 3046510501666004224) is located at $\alpha = 07^{\text{h}} 04^{\text{m}} 37.973^{\text{s}}$, $\delta = -10^{\circ} 43' 37.78''$. The photogeometric distance is estimated to be 870_{-78}^{+66} pc (C. A. L. Bailer-Jones et al. 2021). Based on Gaia data, the object is consistent with a main-sequence star.

¹⁵ <https://snad.space/catalog/>

¹⁶ This object was also independently found using a different approach, Signature Anomaly Detection (E. Gangler et al. 2025).

¹⁴ <https://ztf.snad.space/>

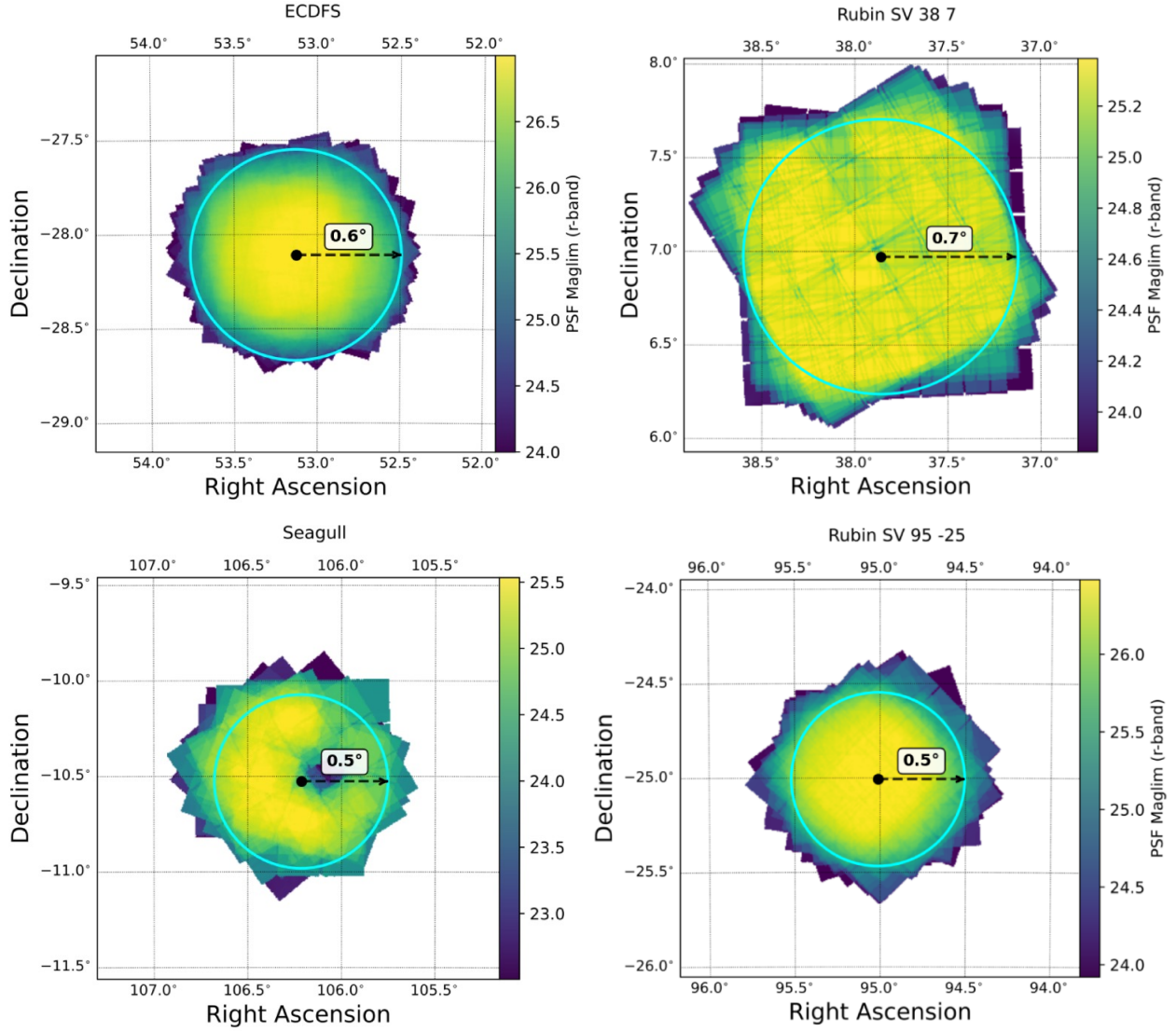


Figure 2. Cumulative imaging depth expressed in terms of the $S/N = 5$ limiting magnitude for unresolved sources for four LSSTComCam fields. We additionally specify a selected radius and corresponding area for each field.

Similar to SNAD273, this object shows signs of solar-type variability (see Fig. 3d).

4.1.5. SNAD278

The ZTF OID 359205300002062 (Gaia DR3 3046437074905139072) is located at $\alpha = 07^{\text{h}} 04^{\text{m}} 41.726^{\text{s}}$, $\delta = -10^{\circ} 54' 26.14''$. The photogeometric distance is estimated to be 1373_{-206}^{+307} pc (C. A. L. Bailer-Jones et al. 2021).

The ZTF folded light curve is shown in Fig. 3e. Based on its photometric properties, specifically, the presence of a distortion wave, an amplitude of ~ 0.6 mag in the zr -band, and flares, we tentatively classify this object as an RS CVn-type variable. The estimated period is $P = 2.03916$ days.

4.1.6. SNAD279

The star ZTF OID 359205300031896 (Gaia DR3 3046431916644875136) is located at $\alpha = 07^{\text{h}} 04^{\text{m}} 45.173^{\text{s}}$, $\delta = -10^{\circ} 59' 50.28''$. The photogeometric distance is estimated to be 1246_{-143}^{+175} pc (C. A. L. Bailer-Jones et al. 2021). According to E. L. Hunt & S. Reffert 2024, it is a member of open cluster Theia 1654.

The ZTF folded light curve is shown in Fig. 3f. Based on its photometric properties, we also interpret the observed brightness modulation as likely caused by stellar spots and rotation, BY Draconis type (BY). The estimated period is $P = 7.11703$ days.

4.2. Classification and determination of light curve parameters of known variables

In this section, we focus on variable objects that have been previously catalogued as variables, mainly using machine learning techniques. For these sources, our newly acquired data allowed us to determine their periods and refine or clarify their variability classifications. This visual re-evaluation provides improved or more precise parameters for known variables, supporting their further study and contributing to the reliability of variable star catalogues.

4.2.1. 452216400002679

The star ZTF OID 452216400002679 (Gaia DR3 19359689641429888) is classified as eclipsing binary (EB) system by Gaia Collaboration (2022). Based on ZTF DR23 data, we revised the period to 1.10166 days, correcting the inaccurate value of 0.54928 days previously reported by Gaia Collaboration (2022). The updated folded light curve is shown in Fig. 4a.

4.2.2. 258207200007316

The star ZTF OID 258207200007316 (Gaia DR3 2912319917858743808) is classified as an RS CVn-type

variable by Gaia Collaboration (2022), although no period is provided there.

According to Gaia DR3 and EDR3 data, this object is a late G- to early K-type main-sequence star, with an effective temperature of $T_{\text{eff}} = 5212_{-21}^{+23}$ K, surface gravity $\log g = 4.11 \pm 0.01$, and moderate metallicity $[\text{Fe}/\text{H}] = -0.37 \pm 0.03$.

Based on its ZTF light curve, we identify clear photometric variability with a well-defined period of 15.9665 days (see folded light curve in Fig. 4b). The absence of signatures indicating binarity or other types of variability suggests that the modulation is most likely due to rotational modulation from stellar spots. We therefore classify this object as a rotational variable (ROT), which with high probability belongs to the BY type.

4.2.3. 258208100007880

The star ZTF OID 258208100007880 (Gaia DR3 2912353727841154688, ATO J094.6486–24.8319) is classified as a close binary in the Atlas survey (A. N. Heinze et al. 2018) and as VAR by AAVSO VSX¹⁷. Based on ZTF DR23 data, we revised the period to 0.690844 days and classified the source as EB. The updated folded light curve is shown in Fig. 4c.

4.2.4. 258208100012201

The star ZTF OID 258208100012201 (Gaia DR3 2912282809341518336, ATO J094.9103–25.1659) is classified as irregular variable star with $P = 18.928$ days by A. N. Heinze et al. (2018) and long periodic variable by Gaia Collaboration (2022).

Based on this period and the shape of the ZTF folded light curve (Fig. 4d), we suggest that the star is likely an ellipsoidal variable in a close binary system, which warrants a revision of its previous classification as an irregular variable.

4.2.5. 359205100018012

The star ZTF OID 359205100018012 (Gaia DR3 3046550595183360000, ZTF J070713.15–103751.6) is classified as a semiregular variable by X. Chen et al. (2020).

The ZTF light curve is shown in Fig. 4e. Its blue color and the morphology of the light curve are consistent with a dwarf nova, yet the variability amplitude is significantly lower than typically observed for that class. Given its photometric properties, we also consider the possibility that it may be eruptive irregular variable of the γ Cassiopeiae type (GCAS).

¹⁷ <https://vsx.aavso.org/index.php?view=detail.top&oid=4468280>

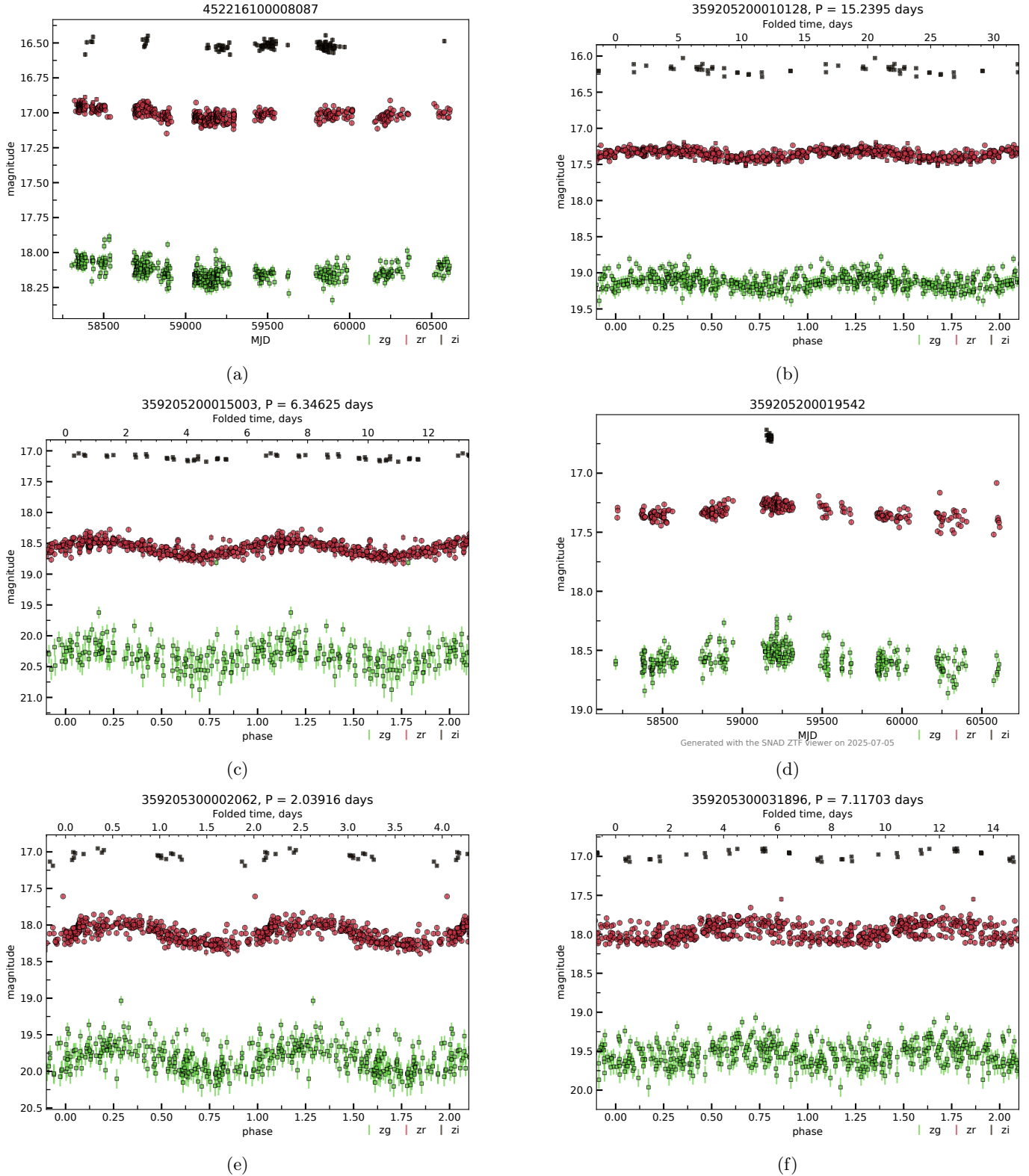


Figure 3. Light curves of eight new ZTF variable stars discovered in LSSTComCam target fields during the SNAD-VIII Workshop. For periodic variables, folded light curves are shown along with the corresponding periods: (a) 452216100008087 (see Section 4.1.1), (b) 359205200010128 (see Section 4.1.2), (c) 359205200015003 (see Section 4.1.3), (d) 359205200019542 (see Section 4.1.4), (e) 359205300002062 (see Section 4.1.5), (f) 359205300031896 (see Section 4.1.6).

Interestingly, this object was also flagged as an anomaly by an Isolation Forest algorithm in the variability-based anomaly search by H.-S. Chan et al. (2022).

4.2.6. 359205200019829

The star ZTF OID 359205200019829 (GDS_J0704458–104418, ATO J106.1908–10.7383) is classified as ROT in T. Jayasinghe et al. (2018) and as a sinusoidal variable (NSINE) by A. N. Heinze et al. (2018); however, no period was previously reported. We determined its period to be 6.20526 days (Fig. 4f). The smooth, low-amplitude, sinusoidal shape of the folded light curve supports its classification as a rotational variable. This interpretation is further supported by the physical parameters from Gaia: $T_{\text{eff}} = 5485_{-111}^{+84}$ K, $\log g = 4.57 \pm 0.02$, and $[\text{Fe}/\text{H}] = -0.67_{-0.10}^{+0.11}$. Together, these characteristics are consistent with a BY variable, where the observed brightness changes are caused by star spots modulated by stellar rotation.

5. CONCLUSIONS

In this work, we presented the results of the SNAD-VIII Workshop, during which we applied the SNAD pipeline to search for anomalous light curves in the Zwicky Transient Facility Data Release 23, focusing on regions of the sky that overlap with the Vera C. Rubin Observatory’s LSSTComCam target fields.

We ran the PineForest active anomaly detection algorithm on four LSSTComCam fields: two galactic (Rubin SV 95–25 and Seagull) and two extragalactic (Rubin SV 387 and ECDFS). In total, we visually inspected 400 ZTF light curves identified as anomalous by the algorithm (1 % of the total number of objects).

As a result, we discovered six previously uncatalogued variable stars, including two showing solar-type variability, two RS CVn candidates, one ellipsoidal variable, and one BY Draconis-type star. These objects have been

added to the SNAD catalog and assigned internal identifiers. In addition to the new discoveries, we also refined the classification and measured accurate periods for six known variable stars.

Our findings show that in ZTF DR23, anomaly detection reveal new and interesting variables. With LSST’s deeper and richer data, we expect to discover many more rare and unusual objects using similar techniques.

ACKNOWLEDGMENTS

This work is a result from the SNAD VIII Workshop¹⁸, which took place in Yerevan, Armenia, from 29 June to 5 July 2025. We acknowledge the support of SberCloud¹⁹ for providing computational resources for the development of this work, and in particular thank Albert Yefimov. We deeply thank Areg Mickaelian and all the staff of the Byurakan Astrophysical Observatory who kindly welcome our team during our stay in Yerevan. We thank Alexandra Zubareva for assistance with the classification of variable stars. M. Pruzhinskaya and E.E.O. Ishida warmly thank Katyusha and Misha for their generous hospitality during our time in Armenia. M. Pruzhinskaya, T. Semenikhin, A. Lavrukhina, M. Kornilov acknowledge support from a Russian Science Foundation grant 24-22-00233, <https://rscf.ru/en/project/24-22-00233/>. The work of V. Krushinsky was supported by a project of youth scientific laboratory, topic FEUZ-2025-0003. E. E. O. Ishida acknowledges support from the 2024 CNRS International Emerging Actions (IEA). Support was provided by Schmidt Sciences, LLC. for K. Malanchev.

Facilities: ZTF (ZTF Team 2025)

Software: Source Extractor (E. Bertin & S. Arnouts 1996), ASTROPY (Astropy Collaboration et al. 2013, 2018, 2022), NUMPY (S. van der Walt et al. 2011), MATPLOTLIB (J. D. Hunter 2007), PANDAS (T. pandas development team 2020; Wes McKinney 2010).

REFERENCES

- Ahumada, R., Allende Prieto, C., Almeida, A., et al. 2020, ApJS, 249, 3, doi: [10.3847/1538-4365/ab929e](https://doi.org/10.3847/1538-4365/ab929e)
- Aleo, P. D., Malanchev, K. L., Pruzhinskaya, M. V., et al. 2022, NewA, 96, 101846, doi: [10.1016/j.newast.2022.101846](https://doi.org/10.1016/j.newast.2022.101846)
- Astropy Collaboration, Robitaille, T. P., Tollerud, E. J., et al. 2013, A&A, 558, A33, doi: [10.1051/0004-6361/201322068](https://doi.org/10.1051/0004-6361/201322068)
- Astropy Collaboration, Price-Whelan, A. M., Sipőcz, B. M., et al. 2018, AJ, 156, 123, doi: [10.3847/1538-3881/aabc4f](https://doi.org/10.3847/1538-3881/aabc4f)
- Astropy Collaboration, Price-Whelan, A. M., Lim, P. L., et al. 2022, ApJ, 935, 167, doi: [10.3847/1538-4357/ac7c74](https://doi.org/10.3847/1538-4357/ac7c74)
- Bailer-Jones, C. A. L., Rybizki, J., Fouesneau, M., Demleitner, M., & Andrae, R. 2021, AJ, 161, 147, doi: [10.3847/1538-3881/abd806](https://doi.org/10.3847/1538-3881/abd806)

¹⁸ <https://snad.space/2025/>

¹⁹ <https://cloud.ru/>

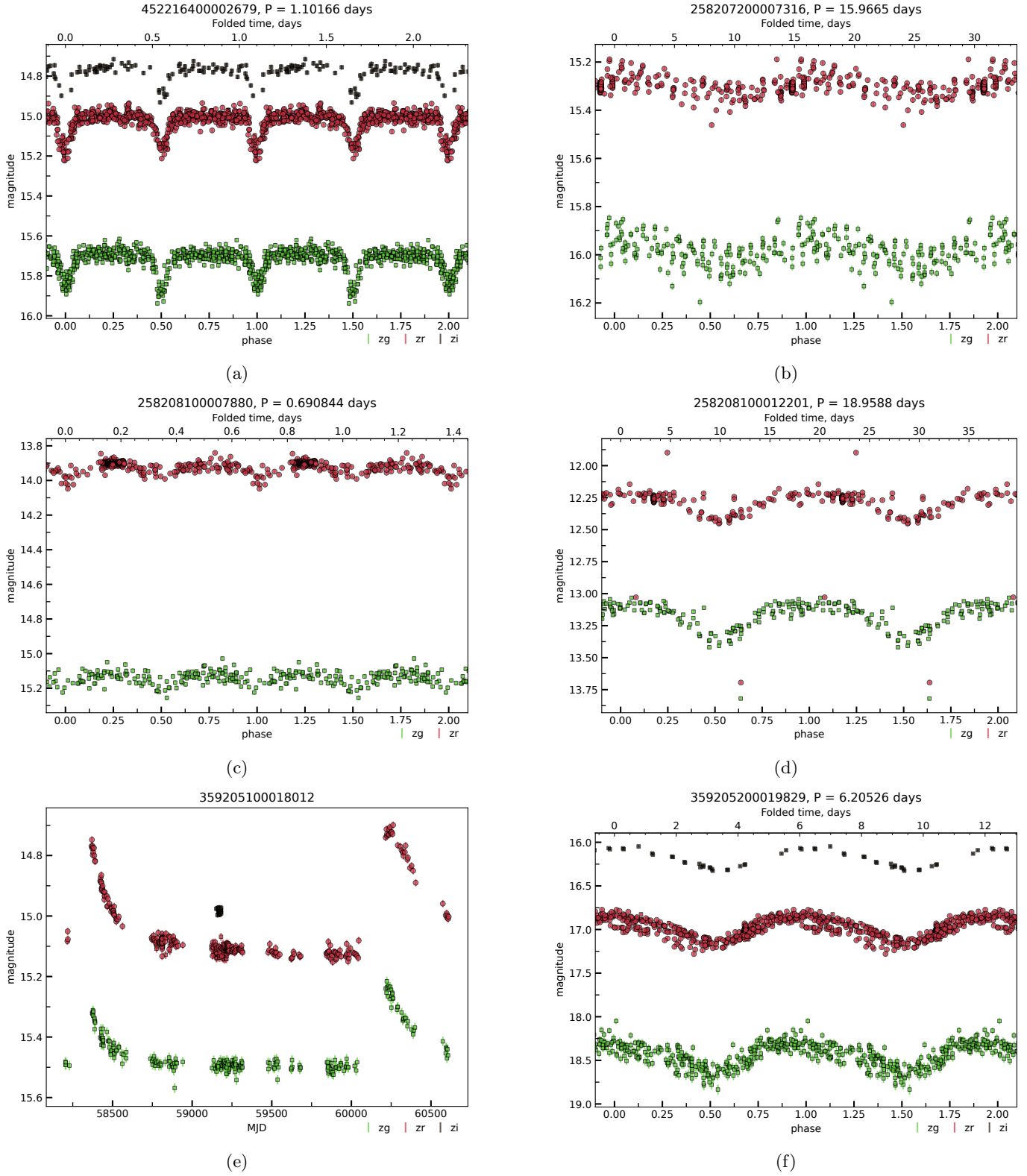


Figure 4. Light curves of catalogued variables for which we refine the classification and/or determine the period: (a) 452216400002679 (see Section 4.2.1), (b) 258207200007316 (see Section 4.2.2), (c) 258208100007880 (see Section 4.2.3), (d) 258208100012201 (see Section 4.2.4), (e) 359205100018012 (see Section 4.2.5), (f) 359205200019829 (see Section 4.2.6).

- Bellm, E. C., Kulkarni, S. R., Graham, M. J., et al. 2019, *PASP*, 131, 018002, doi: [10.1088/1538-3873/aaecbe](https://doi.org/10.1088/1538-3873/aaecbe)
- Bertin, E., & Arnouts, S. 1996, *A&AS*, 117, 393, doi: [10.1051/aas:1996164](https://doi.org/10.1051/aas:1996164)
- Breiman, L. 2001, *Machine learning*, 45, 5
- Carlin, J. L., Ferguson, P. S., Vivas, A. K., Caplar, N., & Malanchev, K. 2025, arXiv e-prints, arXiv:2507.00192, doi: [10.48550/arXiv.2507.00192](https://doi.org/10.48550/arXiv.2507.00192)
- Chambers, K. C., Magnier, E. A., Metcalfe, N., et al. 2016, arXiv e-prints, arXiv:1612.05560, doi: [10.48550/arXiv.1612.05560](https://doi.org/10.48550/arXiv.1612.05560)
- Chan, H.-S., Villar, V. A., Cheung, S.-H., et al. 2022, *ApJ*, 932, 118, doi: [10.3847/1538-4357/ac69d4](https://doi.org/10.3847/1538-4357/ac69d4)
- Chen, X., Wang, S., Deng, L., et al. 2020, *ApJS*, 249, 18, doi: [10.3847/1538-4365/ab9cae](https://doi.org/10.3847/1538-4365/ab9cae)
- Choi, Y., Olsen, K. A. G., Carlin, J. L., et al. 2025, arXiv e-prints, arXiv:2507.01343, doi: [10.48550/arXiv.2507.01343](https://doi.org/10.48550/arXiv.2507.01343)
- Deeming, T. J. 1975, *Ap&SS*, 36, 137, doi: [10.1007/BF00681947](https://doi.org/10.1007/BF00681947)
- Duncan, K. J. 2022, *MNRAS*, 512, 3662, doi: [10.1093/mnras/stac608](https://doi.org/10.1093/mnras/stac608)
- Evans, II, N. J., Dunham, M. M., Jørgensen, J. K., et al. 2009, *ApJS*, 181, 321, doi: [10.1088/0067-0049/181/2/321](https://doi.org/10.1088/0067-0049/181/2/321)
- Flewelling, H. A., Magnier, E. A., Chambers, K. C., et al. 2020, *ApJS*, 251, 7, doi: [10.3847/1538-4365/abb82d](https://doi.org/10.3847/1538-4365/abb82d)
- Gaia Collaboration. 2022, *VizieR Online Data Catalog: Gaia DR3 Part 4. Variability (Gaia Collaboration, 2022)*, *VizieR On-line Data Catalog: I/358*. Originally published in: 2023A&A...674A...1G
- Gaia Collaboration, Vallenari, A., Brown, A. G. A., et al. 2023, *A&A*, 674, A1, doi: [10.1051/0004-6361/202243940](https://doi.org/10.1051/0004-6361/202243940)
- Gangler, E., Ishida, E. E. O., Kornilov, M. V., et al. 2025, arXiv e-prints, arXiv:2506.16314, doi: [10.48550/arXiv.2506.16314](https://doi.org/10.48550/arXiv.2506.16314)
- Guy, L. P., Bechtol, K., Bellm, E., et al. 2025, *Rubin Observatory Plans for an Early Science Program*, doi: [10.5281/zenodo.15558559](https://doi.org/10.5281/zenodo.15558559)
- Heinze, A. N., Tonry, J. L., Denneau, L., et al. 2018, *AJ*, 156, 241, doi: [10.3847/1538-3881/aae47f](https://doi.org/10.3847/1538-3881/aae47f)
- Hunt, E. B., Marin, J., & Stone, P. J. 1966, *Academic press*
- Hunt, E. L., & Reffert, S. 2024, *VizieR Online Data Catalog: Improving the open cluster census. III. (Hunt+, 2024)*, *VizieR On-line Data Catalog: J/A+A/686/A42*. Originally published in: 2024A&A...686A..42H
- Hunter, J. D. 2007, *Computing in Science and Engineering*, 9, 90, doi: [10.1109/MCSE.2007.55](https://doi.org/10.1109/MCSE.2007.55)
- Jayasinghe, T., Kochanek, C. S., Stanek, K. Z., et al. 2018, *MNRAS*, 477, 3145, doi: [10.1093/mnras/sty838](https://doi.org/10.1093/mnras/sty838)
- Kornilov, M. V., Korolev, V. S., Malanchev, K. L., et al. 2025, *Astronomy and Computing*, 52, 100960, doi: [10.1016/j.ascom.2025.100960](https://doi.org/10.1016/j.ascom.2025.100960)
- Lada, C. J., & Lada, E. A. 2003, *ARA&A*, 41, 57, doi: [10.1146/annurev.astro.41.011802.094844](https://doi.org/10.1146/annurev.astro.41.011802.094844)
- Lafler, J., & Kinman, T. D. 1965, *ApJS*, 11, 216, doi: [10.1086/190116](https://doi.org/10.1086/190116)
- Lange, T., Nordby, M., Pollek, H., et al. 2024, in *Proc. SPIE Int. Soc. Opt. Eng., Vol. 13096 (Yokohama, Japan: SPIE)*, 130961O, doi: [10.1117/12.3019302](https://doi.org/10.1117/12.3019302)
- Lavrukhina, A., & Malanchev, K. 2023, *Memorie della Società Astronomica Italiana Journal of the Italian Astronomical Society*, 102
- Liu, F. T., Ting, K. M., & Zhou, Z.-H. 2008, in *2008 Eighth IEEE International Conference on Data Mining*, 413–422, doi: [10.1109/ICDM.2008.17](https://doi.org/10.1109/ICDM.2008.17)
- Loh, W.-Y. 2014, *International Statistical Review*, 82, 329
- Lomb, N. R. 1976, *Ap&SS*, 39, 447, doi: [10.1007/BF00648343](https://doi.org/10.1007/BF00648343)
- LSST Science Collaboration, Abell, P. A., Allison, J., et al. 2009, arXiv e-prints, arXiv:0912.0201, doi: [10.48550/arXiv.0912.0201](https://doi.org/10.48550/arXiv.0912.0201)
- Maíz Apellániz, J., Holgado, G., Pantaleoni González, M., & Caballero, J. A. 2023, *A&A*, 677, A137, doi: [10.1051/0004-6361/202346759](https://doi.org/10.1051/0004-6361/202346759)
- Malanchev, K., Kornilov, M. V., Pruzhinskaya, M. V., et al. 2023, *PASP*, 135, 024503, doi: [10.1088/1538-3873/abc292](https://doi.org/10.1088/1538-3873/abc292)
- Malanchev, K., DeLucchi, M., Caplar, N., et al. 2025, arXiv e-prints, arXiv:2506.23955, doi: [10.48550/arXiv.2506.23955](https://doi.org/10.48550/arXiv.2506.23955)
- Malanchev, K. L., Pruzhinskaya, M. V., Korolev, V. S., et al. 2021, *MNRAS*, 502, 5147, doi: [10.1093/mnras/stab316](https://doi.org/10.1093/mnras/stab316)
- Mowlavi, N., Rimoldini, L., Evans, D. W., et al. 2021, *VizieR Online Data Catalog: Large-amplitude variables in Gaia DR2 (Mowlavi+, 2021)*, *VizieR On-line Data Catalog: J/A+A/648/A44*. Originally published in: 2021A&A...648A..44M doi: [10.26093/cds/vizier.36480044](https://doi.org/10.26093/cds/vizier.36480044)
- NSF-DOE Vera C. Rubin Observatory. 2025, *The Vera C. Rubin Observatory Data Preview 1, Technical Note RTN-095*, Vera C. Rubin Observatory, doi: [10.71929/rubin/2570536](https://doi.org/10.71929/rubin/2570536)
- pandas development team, T. 2020, *pandas-dev/pandas: Pandas, latest Zenodo*, doi: [10.5281/zenodo.3509134](https://doi.org/10.5281/zenodo.3509134)
- Pruzhinskaya, M. V., Ishida, E. E. O., Novinskaya, A. K., et al. 2023, *A&A*, 672, A111, doi: [10.1051/0004-6361/202245172](https://doi.org/10.1051/0004-6361/202245172)

- Roodman, A., Rasmussen, A., Bradshaw, A., et al. 2024, in Society of Photo-Optical Instrumentation Engineers (SPIE) Conference Series, Vol. 13096, Ground-based and Airborne Instrumentation for Astronomy X, ed. J. J. Bryant, K. Motohara, & J. R. D. Vernet, 130961S, doi: [10.1117/12.3019698](https://doi.org/10.1117/12.3019698)
- Samus', N. N., Kazarovets, E. V., Durlevich, O. V., Kireeva, N. N., & Pastukhova, E. N. 2017, *Astronomy Reports*, 61, 80, doi: [10.1134/S1063772917010085](https://doi.org/10.1134/S1063772917010085)
- Samus', N. N., Goranskii, V. P., Durlevich, O. V., et al. 2003, *Astronomy Letters*, 29, 468, doi: [10.1134/1.1589864](https://doi.org/10.1134/1.1589864)
- Scargle, J. D. 1982, *ApJ*, 263, 835, doi: [10.1086/160554](https://doi.org/10.1086/160554)
- Semenikhin, T. A., Kornilov, M. V., Pruzhinskaya, M. V., et al. 2025, *Astronomy and Computing*, 51, 100919, doi: [10.1016/j.ascom.2024.100919](https://doi.org/10.1016/j.ascom.2024.100919)
- Sokolovsky, K. V., & Lebedev, A. A. 2018, *Astronomy and Computing*, 22, 28, doi: [10.1016/j.ascom.2017.12.001](https://doi.org/10.1016/j.ascom.2017.12.001)
- Sreejith, S., Pruzhinskaya, M. V., Volnova, A. A., et al. 2025, arXiv e-prints, arXiv:2504.08053, doi: [10.48550/arXiv.2504.08053](https://doi.org/10.48550/arXiv.2504.08053)
- van der Walt, S., Colbert, S. C., & Varoquaux, G. 2011, *Computing in Science and Engineering*, 13, 22, doi: [10.1109/MCSE.2011.37](https://doi.org/10.1109/MCSE.2011.37)
- Volnova, A. A., Aleo, P. D., Lavrukhina, A., et al. 2024, in *Data Analytics and Management in Data Intensive Domains*, ed. J. Baixeries, D. I. Ignatov, S. O. Kuznetsov, & S. Stupnikov (Cham: Springer Nature Switzerland), 195–208
- Voloshina, A. S., Lavrukhina, A. D., Pruzhinskaya, M. V., et al. 2024, *Monthly Notices of the Royal Astronomical Society*, 533, 4309, doi: [10.1093/mnras/stae2031](https://doi.org/10.1093/mnras/stae2031)
- Watson, C. L., Henden, A. A., & Price, A. 2006, *Society for Astronomical Sciences Annual Symposium*, 25, 47
- Wes McKinney. 2010, in *Proceedings of the 9th Python in Science Conference*, ed. Stéfan van der Walt & Jarrod Millman, 56 – 61, doi: [10.25080/Majora-92bf1922-00a](https://doi.org/10.25080/Majora-92bf1922-00a)
- ZTF Team. 2025, *ZTF Objects Table*, IPAC, doi: [10.26131/IRSA597](https://doi.org/10.26131/IRSA597)